Deciphering multivalent glycocluster–lectin interactions through AFM characterization of the self-assembled nanostructures

Francesca Zuttion, Delphine Sicard, Lucie Dupin, Gérard Vergoten, Camille Girard-Bock, Mimouna Madaoui, Yann Chevolot, François Morvan, Sébastien Vidal, Jean-Jacques Vasseur, et al.

HAL Id: hal-02325343

https://hal.science/hal-02325343

Submitted on 23 Nov 2020

Journal Name

ARTICLE

Deciphering multivalent glycocluster-lectin interactions through AFM characterization of the self-assembled nanostructures

Francesca Zuttion*[a], Delphine Sicard*[a†], Lucie Dupin[a], Gérard Vergoten[b], Camille Girard-Bock[a††], Mimouna Madaoui[c], Yann Chevolot[a], Francois Morvan[c], Sébastien Vidal[d], Jean-Jacques Vasseur[c], Eliane Souteyrand[a] and Magali Phaner-Goutorbe[a]

Pseudomonas aeruginosa is a human opportunistic pathogen responsible for lung infections in cystic fibrosis patients. The emergence of resistant strains and its ability to form a biofilm seems to give a selective advantage to the bacterium and thus new therapeutic approaches are needed. To infect lung, the bacterium uses several virulence factors, like LecA lectins. These proteins are involved in bacterial adhesion thanks to their specific interaction with carbohydrates of the host epithelial cells. The tetrameric LecA lectin specifically binds galactose residues. A new therapeutic approach is based on the development of highly affine synthetic glycoclusters able to selectively link with LecA to interfere the natural carbohydrate-LecA interaction. In this study, we combined Atomic Force Microscopy imaging and Molecular Dynamics simulations to visualize and understand the arrangements formed by LecA and five different glycoclusters. Our glycoclusters are small scaffolds characterized by a core and four branches, which terminate by a galactose residue. Depending on the nature of the core and the branches, the glycocluster-lectin interaction can be modulated and the affinity increased. We show that glycocluster-LecA arrangements highly depend on the glycocluster architecture: the core influences the rigidity of the geometry and the directionality of the branches, whereas the nature of the branch determines the compactness of the structure and the ease of the binding.

Introduction

The human opportunistic pathogen *Pseudomonas aeruginosa* (PA) is a Gram-negative bacterium which causes chronic infections and degradation of the respiratory tract of cystic fibrosis and immune-compromised patients[1]. This bacterium is resistant against conventional antibiotic therapies[2] due to the emergence of highly resistant strains[3] and its ability to develop biofilms. The bacteria take advantage of the malfunctioning of the host defenses to use an arsenal of virulence factors which are involved in the adhesion, colonization and infection processes. As a consequence, great efforts have been devoted towards the development of new therapeutic approaches targeting PA virulence factors, including those involved in biofilm formation[4]. Among them, two lectins, LecA and LecB,

were identified as potential therapeutic targets due to their role in cell recognition, biofilm formation and cohesion[5]. In particular, LecA (**Fig. 1a**) is a tetrameric lectin characterized by four identical units. Each of them presents a Carbohydrate Recognition Domain (CRDs) that allows the specific binding to one D-galactose residue (Gal). The binding between the CRD of the lectin and the residue is mediated by hydrogen bonds, hydrophobic contacts, and coordination with a calcium ion (**Fig. 1a**, purple spheres)[6]. The natural ligand of LecA has been identified as the globotriaosylceramide Gb3, which is highly present in human epithelial cells[7].

In order to inhibit the natural interaction between the lectin and the ligand of host cells[8], it has been shown that certain galactosylated glycoclusters have a high selective affinity with LecA[8, 9] due to their multivalency[10] and the so called "glycoside cluster effect"[8, 10]. Their inhibition effect on the activity of lectin-induced PA lung infections has been demonstrated in animal model and represents a promising therapeutic strategy against such bacterial infections[11].

To follow this therapeutic approach, our collaborative group has synthesized more than 150 different glycoclusters[4, 8, 12-18]. Different strategies to build these scaffolds were explored but most of them present a core with multiple branches terminated by a Gal residue capable of interacting with LecA's CRD. The design of the core and the branches are key parameters for achieving optimal topologies toward a maximal cluster effect[13, 14, 19].

In the present study, Atomic Force Microscopy (AFM) was chosen to observe at the nanoscale the arrangement formed by five different glycoclusters when bound to LecA. In addition, Nanosecond Molecular Dynamics (MD) Simulations were performed to better understand these arrangements. The data were analyzed taking into account the values of the dissociation constants (K_d) and the stoichiometry numbers (n) obtained by Isothermal Titration Calorimetry (ITC), in order to find a link between the morphology of the structures, the nature of the glycoclusters (core and branch) and the affinity to LecA.

Name	Core	Branches		Termination	n	K_d (nmol/L)
		Linker 1	Linker 2			
C1	Calix[4]-arene	OMTz	EG$_3$	Galactose	0.24	170
P1	Porphyrin	OMTz	EG$_3$	Galactose	0.46	330
M1	Mannose	POProTz	EG$_3$	Galactose	0.28	11000
M2	Mannose	POProTz	AcNPh	Galactose	0.46	194
M3	Mannose	POEG2MTz	AcNPh	Galactose	0.52	157
M4	Mannose	POEG2MTz	AcNPh	Glucose	No Interaction	No Interaction

Table 1: Structural composition of glycoclusters under study. Stoichiometry values n and dissociation constants K_d were determined by ITC to estimate the affinity with LecA. Pro = $CH_2CH_2CH_2$; Tz = triazole $C_2H_1N_3$; EG$_3$ = $(CH_2CH_2O)_3$; Ac = $COCH_2$; M = CH_2; Ph = phenyl, PO = phosphodiester P(=O)(O-)O.

Experimental

Glycoclusters

The six glycoclusters used in this study are presented in **Table 1** and their final structures are shown in the Supporting Information. Glycoclusters synthesis was extensively described in References[20, 21], as well as the anti-adhesive properties of C1 and M3 on *in vitro* biofilm assays[11,20]. They are characterized by a core, four branches formed with two different linkers. The branches are ended by one monosaccharide residue.

AFM Imaging

As previously described[22, 23], the LecA-glycocluster complexes were prepared in vitro by mixing 20 µL of CaCl$_2$ (final concentration 0.3 µmol/L), 10 µL of LecA (final concentration 25 pmol/L) and 10 µL of glycocluster (final concentration 25 pmol/L). The complex was prepared with the same proportion of lectin and glycocluster (1:1) to favor the binding of one galactose residue to each CRD of the lectins. It was shown by ITC measurements that the complex forms in solution in the early stage of the titration process and this low concentration of 25 pmol/L was chosen to avoid the creation of large aggregates[24]. Then, the solution was incubated 1 hour at room temperature. Finally, 20 µL of the final solution were deposited on freshly cleaved mica surface and dried overnight in a desiccator at room temperature and ambient pressure. Topographic images were acquired in air and at room temperature, using a SMENA B (NT-MDT, Russia) AFM microscope in Amplitude Modulation (AM) AFM mode with triangular cantilevers (NSC 21 from MikroMasch, Bulgaria) having a tip radius of 10 nm. The data analysis was performed with Gwyddion Software. By adjusting amplitude ratio, it is possible to image these soft molecules without damaging them[25]. Measurements were performed in air for two main reasons: (*i*) the adsorption of the lectin on mica may not be strong enough to allow to image in liquid, and (*ii*) to ensure the highest resolution conditions to correlate the morphology as observed by AFM and the simulation results. The only artefact derived from this choice is the detection of a smaller height of the complexes, as previously described by Sicard *et al*[22].

Computer Simulations

Simulations were carried out by combining Monte Carlo method[26] with SPASIBA (Spectroscopic Potential Algorithm for Simulating Bimolecular conformational Adaptability)[27, 28] force field that is characterized by the combination of AMBER Van der Waals, electrostatic interactions and Urey-Bradley-Shimanouchi terms for bond stretching, valence angle bending and torsional parameters. Monte Carlo simulations were run to minimize the energy of the complex and find the most probable conformations. The protein structures were considered as aggregates and the final assembly was optimized with all atoms released by applying the SPASIBA force field by means of molecular docking. The interaction potential energies (ΔE) of the possible arrangements were calculated by the difference between the energy of the complex ($E_{complex}$) and the energies of both the protein ($E_{protein}$) and the ligand (E_{ligand}) independently, as shown in equation (1):

$$\Delta E = E_{complex} - (E_{protein} + E_{ligand}) \qquad (1)$$

ΔE values were used to evaluate the more energetically stable structures. The LecA lectin structure file was retrieved from the RCSB Protein Data Bank website (PDB code 4LJH, since it shows

Journal Name

ARTICLE

the Gal molecules in the CDRs of the lectin). Molecular graphics and analysis were performed using the Discovery Studio Visualizer 4.0 Software (Accelrys, San Diego, CA, USA).
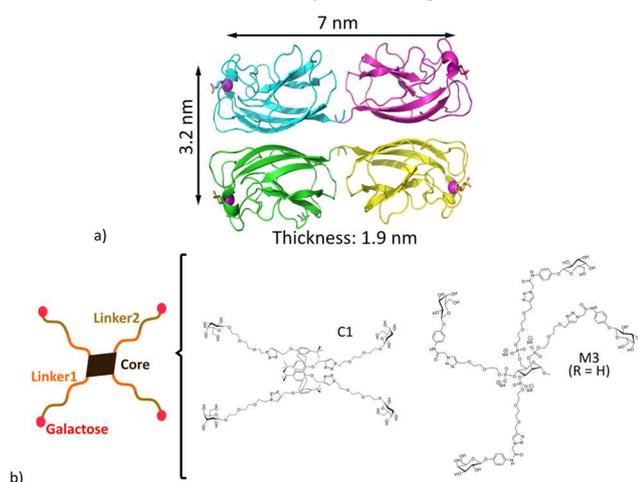

Figure 1: (a) Crystal structure of LecA complex with GalA-QRS at 2.31 Å resolution (RCBS code 4LKD, https://www.rcsb.org/structure/4LKD); (b) Schematic of the general structure of the glycoclusters and two examples of the glycoclusters studied, namely C1 and M3. All the structures are given in the Supporting Information.

Results and discussion

LecA-glycocluster affinity

LecA lectin has a cobblestone shape of 7.0 x 3.2 x 1.9 nm^3 with four identical CRDs which recognize specifically galactose residue, as shown in **Fig. 1a**. In order to understand the relationship between the glycocluster structural composition, the LecA-glycocluster affinity and the LecA-glycocluster complexes arrangement, five tetravalent glycoclusters, called as C1, P1, M1, M2 and M3 (**Table 1**), were selected for their affinity with the lectin[20, 21]. These synthesized molecules are composed by a core, two linkers, named here linker 1 and linker 2, forming the branches, and to finish a monosaccharide residue, in this case one galactose to interact with LecA (schematic drawing in **Fig. 1b**). On one side, three of them, C1, P1 and M1, present different cores but similar branches composed by two linkers: oxymethylenetriazole (OMTz) or phosphodiester propyl-triazole chain (POProTz) as linker 1 and a hydrophilic triethyleneglycol (EG$_3$) as linker 2. The difference in length of the alkyl chain between POPro and OM compensates the difference in core size: a calix[4]arene for C1, a porphyrin for P1 and a mannose for M1[20, 24]. On the other side, M1, M2 and M3 have the same mannose core but different branches. In M2,

linker 1 is the same as in M1 (POProTz) and linker 2 is the same as in M3: a rigid aromatic acetamidephenyl (AcNPh), while, the linker 1 in

M3 is a flexible phosphodiester diethyleneglycol methylene triazole (POEG$_2$MTz)[21]. Additionally, M4 presents the same core and branches than M3 glycocluster but exhibits glucose as terminal carbohydrate residue. It was used as a negative control since glucose does not interact with LecA.

Thermodynamic parameters including the stoichiometry value (n) and the dissociation constant (K_d) of the interaction with the lectin have been obtained by ITC [20,21,29] and presented in **Table 1**. The stoichiometry value indicates the number of binding between one glycocluster and the monomers of the lectin. Depending on the glycocluster structure, n values are close to 0.5 or 0.25. . This indicates that one glycocluster can bind up to two lectin monomers for n = 0.5 (1:2), or to four monomers for n = 0.25 (1:4), without excluding the less probable intermediate case n = 0.33 (1:3, interaction with three monomers). For the five glycoclusters here studied, the n values were previously estimated at: n = 0.24 for C1, n = 0.28 for M1, n = 0.46 for P1 and M2 and n = 0.52 for M3, leading to different possible topologies when interacting with LecA. The dissociation constant K_d refers to the affinity of the lectin-glycocluster interaction: the lower the K_d the stronger the interaction. In this case, the dissociation constants were determined at: K_d = 170 nmol/L for C1-LecA, K_d = 194 nmol/L for M2-LecA and K_d = 157 nmol/L for M3-LecA. The K_d increases to K_d = 330 nmol/L for the P1-LecA and reaches the highest value of K_d = 11000 nmol/L for M1-LecA (**Table 1** and [20, 21]).

Effect of the core on nanostructures

Fig. 2 presents three AFM images of the complexes C1-LecA, P1-LecA and M1-LecA, respectively, created in solution and deposited on a mica surface. These three glycoclusters have roughly the same branch, a phosphodiester propyltriazole (POProTz) or a oxymethylenetriazole (OMTz) as linker 1 and the same flexible triethyleneglycol (EG$_3$) arm as linker 2. As the images clearly show, the change in the nature of the core of the three glycoclusters leads to different arrangements formed with LecA:

- A mostly mono-dimensional arrangement with the calix[4]arene-centered glycocluster C1, where alternate lectins and C1 glycoclusters are observed in single filaments. In a previous work, we showed that lectins can be identified along the filament on high resolution images[22].
- A smaller curved structure with larger holes is obtained with the porphyrin core glycocluster P1, in which the width of the sinusoidal branches vary from

40 nm to 125 nm suggesting that one to five lectins can be involved, taking into account the tip convolution[30].

- A large 2D organized lacy structure is found in presence of the mannose-centered glycocluster M1, where sometimes holes can be identified in the arrangement.

The average height of the structures is around 1.4 ± 0.2 nm on all the images. This value is slightly lower than the width of a single lectin measured by crystallography (see **Fig. 1a**), and

previously evidenced by AFM[23]. It seems that the lectins are lying flat on the mica surface, creating 1D or 2D arrangements. The lowering of the size can be attributed to the sample preparation protocol (dried overnight in dessicator)[22, 23] and the adsorption of the protein on the mica surface [31].

To understand the topological arrangement of the obtained complexes, MD simulations have been performed taking into account the stoichiometry *n* values (**Table 1**), which differs from one glycocluster to another. The molecular models,
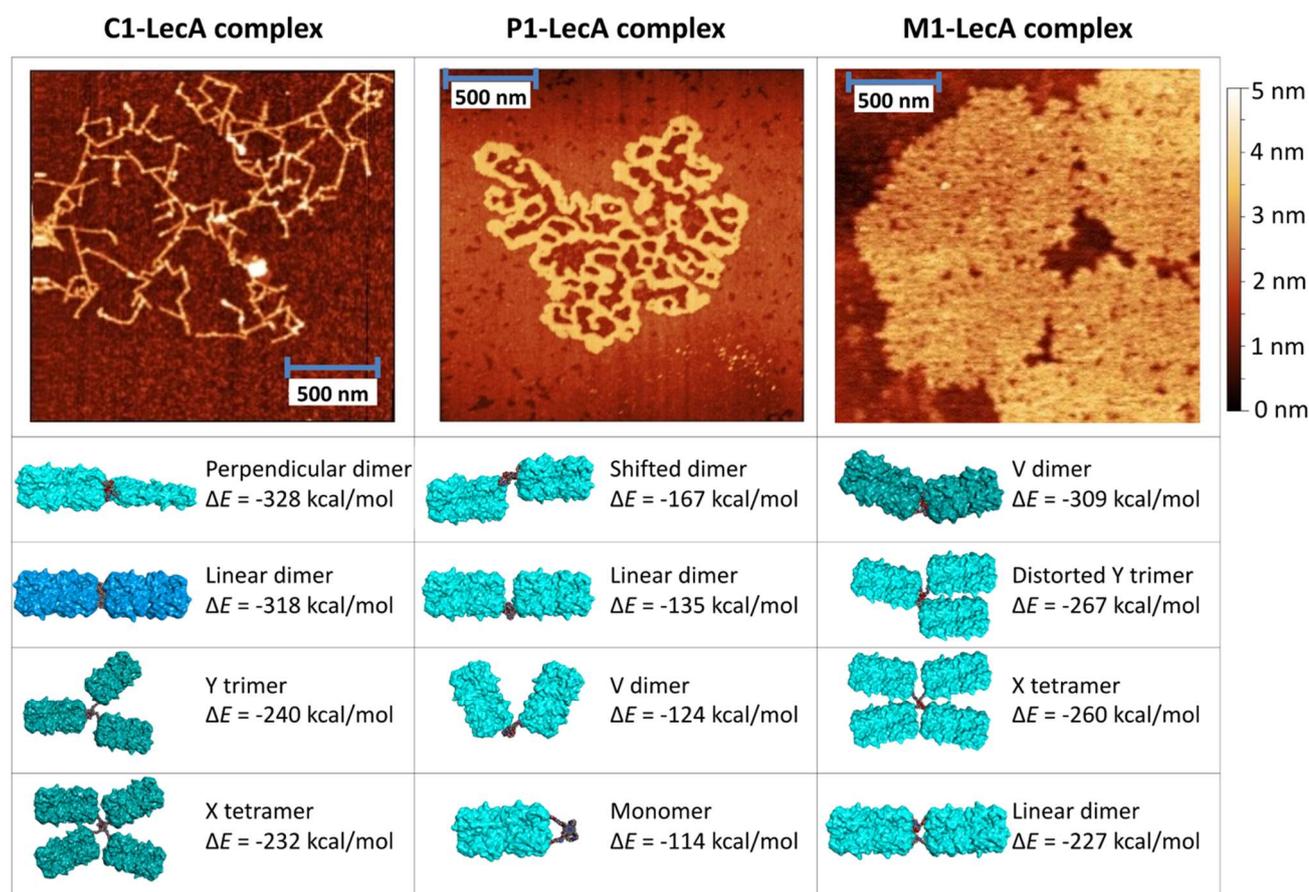

C1-LecA complex	P1-LecA complex	M1-LecA complex
Perpendicular dimer ΔE = -328 kcal/mol	Shifted dimer ΔE = -167 kcal/mol	V dimer ΔE = -309 kcal/mol
Linear dimer ΔE = -318 kcal/mol	Linear dimer ΔE = -135 kcal/mol	Distorted Y trimer ΔE = -267 kcal/mol
Y trimer ΔE = -240 kcal/mol	V dimer ΔE = -124 kcal/mol	X tetramer ΔE = -260 kcal/mol
X tetramer ΔE = -232 kcal/mol	Monomer ΔE = -114 kcal/mol	Linear dimer ΔE = -227 kcal/mol

Figure2: AFM topographic images and MD simulations of C1-LecA, P1-LecA and M1-LecA complexes. Image size: 2 x 2 μm^2.

corresponding to the four more energetically stable structures obtained with one glycocluster and LecA, are presented in **Fig.2** for the three complexes C1-LecA, P1-LecA and M1-LecA.

In particular, for the C1-LecA complex, the more energetically stable structures are obtained with one glycocluster bound to two lectins. This binding leads to two equally favorable possible configurations. The former presents an energy of ΔE = -328 kcal/mol and the lectins are maintained in a 90° orientation one to the other since the four branches of the glycocluster are alternated pointing upwards and downwards around the core structure, resulting in perpendicular planes[22, 32]. In the latter, with a potential energy ΔE = -318 kcal/mol, the two lectins are maintained in a 0º orientation by the glycocluster, leading to a

filament structure where the two lectins are bound to the glycocluster from the same edge. These configurations are respectively 88 kcal/mol and 78 kcal/mol below the value of the third one (ΔE = -240 kcal/mol), where the glycocluster binds three CRDs from three different lectins, leading to a "Y trimer" arrangement of the lectins on the plane. This organization and the one that involves the binding of one glycocluster with four different lectins ("X tetramer", ΔE = -232 kcal/mol) are less favorable. They allow the formation of defects in the structure, such as the bifurcations seen in the AFM images[22]. Therefore, we can evidence that, for C1 glycocluster, the stiffness of the core reinforces the rigidity of the complex while the branches alignment leads to the creation of a 1D filament structure.

For the P1-LecA complex, the stoichiometry is 0.46 close to a 1 glycocluster for 2 CRDs. The four more probable models are characterized by potential energies spanning from ΔE = -167 kcal/mol to ΔE = -114 kcal/mol. This leads to a general shape of the arrangements less constrained, with rounding filaments connected at some places in 2D structures. The porphyrin core is less rigid than the calix[4]arene and the branches present more degrees of freedom. We can consider that in the solution before deposition, the branches can orient themselves more freely with respect of the CRDs of the lectins. The spreading of the structure seems to be limited by the fourth most probable model ("Monomer", ΔE = -114 kcal/mol, **Fig. 2**), where two galactoses of the same glycocluster bind two CRDs of the same lectin.

For the M1-LecA complex, the models correspond to the interaction between four galactoses of the glycocluster and two, three or four lectins (including one or two CRDs per lectin), leading to dimer, trimer and tetramer dispositions, respectively. A mixture of these organizations seems to be responsible of the final architecture of the complex. The structures extend laterally over several hundreds of nanometers forming a compact arrangement with only some holes of different size, being the biggest arrangement of around 300 x 300 nm^2. This means that lectins are close together and might also interact with each other[23]. The geometry is also favored by the flexibility of the mannose core, which authorizes a great degree of freedom to the branches in solution.
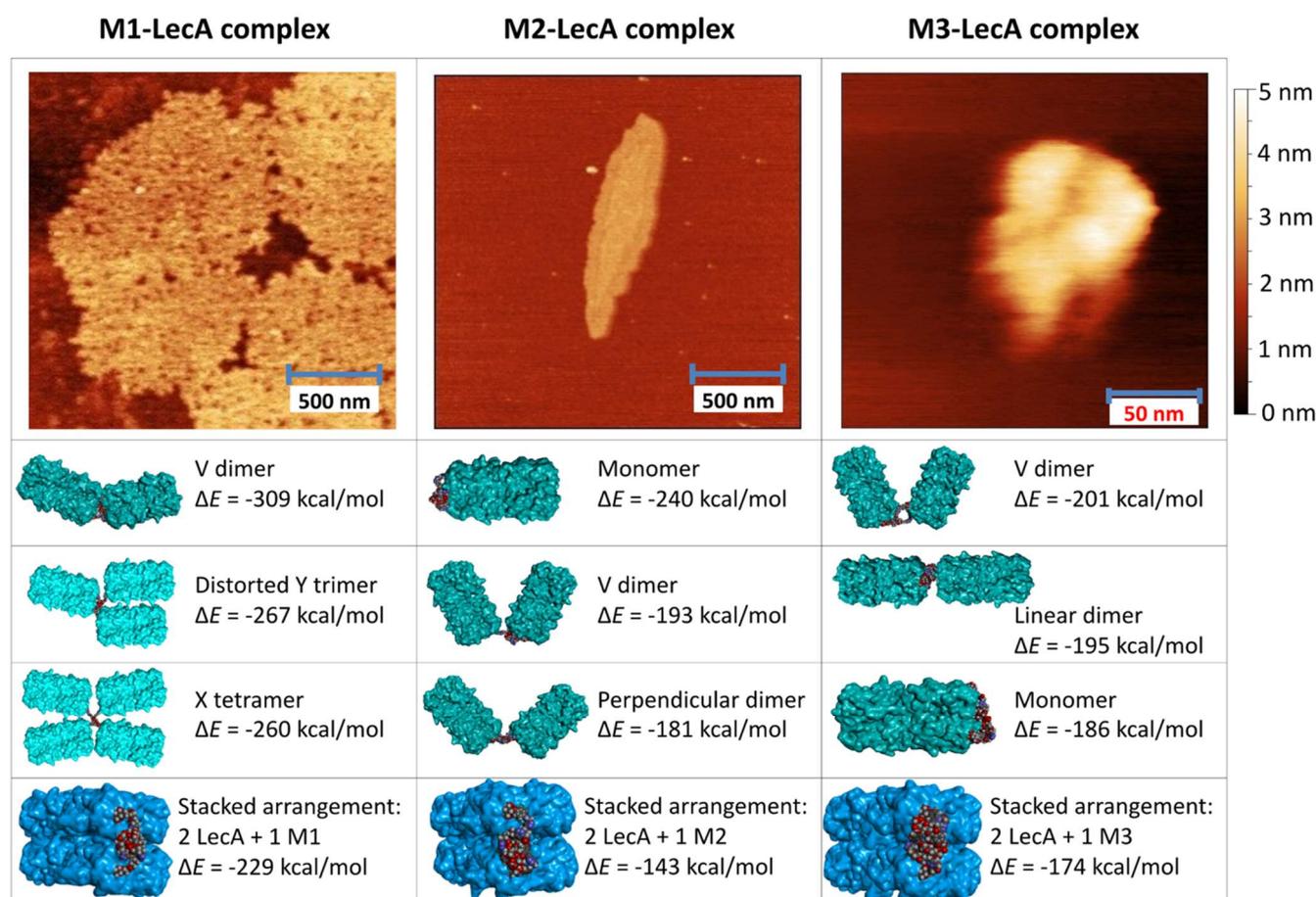

Figure3: AFM topographic images and MD simulations of M1-LecA, M2-LecA and M3-LecA complexes. Image size: 2 x 2 μm^2 for M1-LecA and M2-LecA; 0.2 x 0.2 μm^2 for M3-LecA.

Effect of the branches on nanostructures

To study the influence of the branches on the complex arrangements, three glycoclusters with the same mannose core but different branches were imaged by AFM (**Fig. 3**). The branches differ from each other by the nature of the linker 1 and/or linker 2 (**Table 1**). Also in this case, different nanostructures were observed by AFM, as shown in **Fig. 3**. The

first glycocluster M1 has been previously discussed. M2 and M3 have a higher affinity to LecA than M1 and similarly to C1- and P1-LecA affinity. Their interactions with LecA lead to the formation of smaller and more compact structures. For M2-LecA complex, the small structures are sometimes elongated with well-defined borders characterized by rectangular kinks that would remind the shape of the lectin. Instead, in the case

of M3-LecA complex, the structures are quite small with a size of 70 to 100 nm. These arrangements present also a huge heterogeneity about the structure height that ranges from 1.4 to 25 nm, meaning that the lectins are stacked one over the other at some places (data not shown).

The potential energies of stacked arrangements have been calculated for the three mannose-centered complexes. A value of ΔE = -229 kcal/mol was obtained for M1-LecA, when two stacked lectins are linked to one glycocluster. Even if this energy value is not so far from the one obtained for plane-arrangements, AFM images and the height of M1-LecA complexes arrangement did not evidence such stacked structures. Only small brighter spots on the large 2D monolayer structures appear at some places. In the case of M2 glycocluster, the most energetically favorable arrangements are characterized by the interaction between two galactoses of the glycocluster and two CRDs of two or one lectins, leading to dimer and monomer dispositions respectively. The monomer arrangement can explain why the structures obtained with AFM are so small. We can assume that this monomer configuration blocks the extension of the structure in the plane, leading to small complexes. The stacked arrangement is at 97 kcal/mol from the monomer model, which does not really favor 3D structures formation compared to 2D compact arrangements.

The M3 glycocluster leads roughly to the same behavior as observed with M2. Thus, the most energetically favorable arrangements are characterized by the interaction between two galactoses of the glycocluster and two CRDs of one or two different lectins. The monomer configuration is only at 15 kcal/mol from the most energetically favorable model, explaining the small lateral size of the structures. In addition, the stacked configuration is only at 27 kcal/mol far from the most energetically favorable arrangement, thus it can well explain why some 3D complexes were found. Moreover, these two glycoclusters present roughly the same stoichiometry value (n = 0.52 for M2 and n = 0.46 for M3) and similar low K_d, 194 nmol/L and 157 nmol/L for M2-LecA and M3-LecA, respectively. Once again, it appears that the structures are limited in lateral size for small K_d, with a high affinity between LecA and the glycoclusters.

Influence of lectin/lectin interaction

Due to the drying process, stacked structures appeared and therefore, we cannot exclude the presence of a lectin-lectin interaction. Consequently, one issue arises: how can the lectin-lectin interaction influence the complex formation? To answer this question, the complex formed between the lectin and M4 glycocluster (**Table 1**) was studied. The M4 glycocluster has the same structure than M3 but instead of having galactose residues, it presents glucose that does not interact with LecA.

Cause of the lack of affinity with the lectin, the M4-LecA complexes should be mostly driven by the lectin-lectin interactions. Extended 2D monolayer complexes similar to the ones obtained with M1 were observed by AFM (**Fig. 4**). Thus, the interplay between the glycocluster-lectin and the lectin-lectin interactions must govern the formation of these complexes. MD simulations of lectin-lectin interactions shows

that the scheme with a direct edge-contact between lectins leading to an ΔE = -98 kcal/mol is not negligible and can explain the lateral extension of the structures.

This study contributes to new findings to understand the relation between lectin-glycocluster interaction and the structure of these formed complexes. Hence, five glycoclusters were selected to study the arrangement of the glycoclusters-mediated self-assembly with LecA, since they have different topologies and/or their interaction with LecA exhibited different stoichiometry as determined by ITC. Therefore, we do expect their interaction with LecA to be governed by different mechanisms that could be deciphered by characterizing the resulting nanostructures. In particular, the effects of the core and the branches on the nanostructures have been studied by comparing the arrangement formed with the different glycoclusters. Mainly, the comparison of the C1-LecA, P1-LecA and M1-LecA complexes can show the influence of the core on the complex arrangement, since C1, P1 and M1 have the same branches but different cores. Whereas, the comparison of M1-LecA, M2-LecA and M3-LecA nanostructures can elucidate the influence of the branch as M1, M2 and M3 are mannose-centered glycoclusters with different branches.
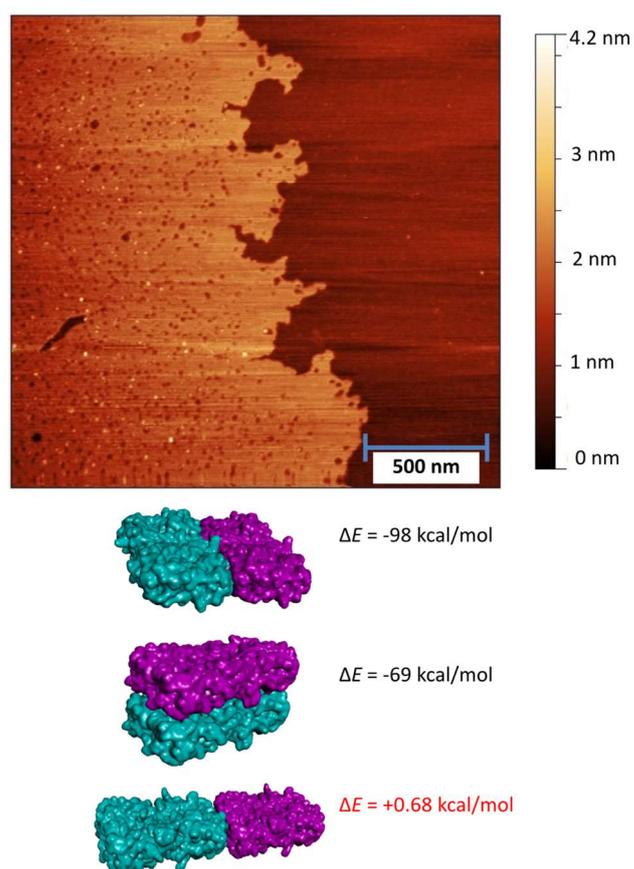

ΔE = -98 kcal/mol

ΔE = -69 kcal/mol

ΔE = +0.68 kcal/mol

Figure 4: AFM topographic image of M4-LecA complex, image size 2 x 2 μm^2 and MD simulation of lectin/lectin interaction.

Due to its nanoscale resolution[33, 34], AFM is a powerful tool to directly visualize these supramolecular arrangements. It allows discriminating small features like single lectins inside a

complicated architecture such as the LecA-glycocluster complexes[22, 23]. However, in most cases, structures are dense and form compact networks that cannot be easily attributed to a specific type of interaction (1:2, 1:3 or 1:4) due to the complexity of the binding modes. Therefore, nanosecond MD simulations, in which ΔE values were used as parameters to evaluate the more energetically stable structures, have been performed to have a better understanding of the glycocluster-LecA arrangements.

By comparing the structures formed with C1, P1 and M1 (different cores), it seems that the geometry of the nanostructures is governed by the nature and the rigidity of the core. The glycocluster C1 has the stiffest core and the highest affinity towards LecA. It leads to the less extended nanostructure while M1 and P1 allow forming less compact (wider) structures. For the structures obtained with the three mannose-centered glycoclusters, it appears that the morphology of the complexes depends more on the linker 2, which is in charge of the accessibility of the galactose residue to the lectin CRD, rather than the linker 1 close to the core. In fact, M1 has the same core and the same linker 1 than M2. The difference in linker 2 leads to a totally different organization of the complex. Unlike the linker 2 for M1, which is characterized by a flexible EG_3 group, the linker 2 for M2 and M3 is an aromatic group which presents a phenyl aglycon able to interact, via a CH-π interaction, with the amino acid (Histidine 50) located close to the CRD of the lectin[35]. This interaction leads to an increased affinity, characterized by a dissociation constant 56 (M2 vs. M1) to 70 (M2 vs. M1) times lower. Moreover, the nature of the linker 2 is likely responsible of the compactness of the M2-LecA and M3-LecA complexes.

In the case of high affinity glycoclusters, the complex formation is mainly driven by the glycocluster-lectin interaction, such as for M2 and M3 glycoclusters, whereas if the affinity of the glycocluster for the lectin is decreased, the lectin-lectin interaction competes with the lectin-glycocluster interaction for the complex formation, as for M1. These results are also in agreement with what was previously found for the lectin-lectin interaction[23]. Lectins alone can interact with each other forming long isolated 2D objects of an average height of 1.5 ± 0.4 nm. The interaction appears to be mainly longitudinal at low lectin concentration (50 nmol/L), as observed by X-ray crystallography and evidenced by AFM[23]. 3D aggregations are less probable. Therefore, lectin complexes seem mostly characterized by lectin-lectin interactions with a direct edge-contact as shown by MD, since stacked interactions would have been related to the formation of piled structures, characterized by a height bigger than 1.5 nm.

Conclusions

In conclusion, these AFM studies combined to MD simulations revealed that the core rigidity and the nature of the linker 2 influence drastically the morphology of the glycocluster-lectin complexes. A relation between the affinity of glycocluster-LecA interaction and the morphology at the nanoscale of the created complexes could be established. A high affinity (K_d around 100

to 200 nmol/L) leads to small structures, compact for M2 and M3, sometimes 3D or limited to the size of the lectin as for C1. When the affinity decreases, the structures extend laterally to large 2D monolayers, observed for M1 and M4. In that case, the lectin-lectin interaction should be taken into account in the process of complex formation. For M1, it competes with the glycocluster-lectin interaction. P1 glycocluster, with an affinity of K_d = 330 nM, presents very specific morphology in between the one obtained for C1 and M1. In ongoing projects, M3 glycocluster was chosen for AFM spectroscopic measurements at the molecular level to quantify the lectin-M3 interaction, and also at the cell level to evaluate its anti-adhesive effect on the adhesion of *Pseudomonas aeruginosa* bacteria to host cells[36]. As a future perspective, to better understand the lectin-glycocluster arrangements, the correlation between nanometric structural description and local chemical information is foreseen by means of AFM-IR[37].

Conflicts of interest

There are no conflicts to declare.

Acknowledgements

Notes and references

1.   N. Floret, X. Bertrand, M. Thouverez and D. Talon, *Pathol Biol (Paris)*, 2009, **57**, 9.
2.   C. Formosa, M. Grare, E. Jauvert, A. Coutable, J.B. Regnouf-de-Vains, M. Mourer, R.E. Duval and E. Dague, *Sci Rep*, 2012, **2**, 575.
3.   T. Strateva and D. Yordanov, *J Med Microbiol*, 2009, **58**, 1133.
4.   S. Wagner, R. Sommer, S. Hinsberger, C. Lu, R.W. Hartmann, M. Empting and A. Titz, *J Med Chem*, 2016, **59**, 5929.
5.   S.P. Diggle, R.E. Stacey, C. Dodd, M. Camara, P. Williams and K. Winzer, *Environ Microbiol*, 2006, **8**, 1095.
6.   A. Imberty, M. Wimmerova, E.P. Mitchell and N. Gilboa-Garber, *Microbes Infect*, 2004, **6**, 221.
7.   B. Blanchard, A. Nurisso, E. Hollville, C. Tetaud, J. Wiels, M. Pokorna, M. Wimmerova, A. Varrot and A. Imberty, *J Mol Biol*, 2008, **383**, 837.
8.   A. Imberty, Y.M. Chabre and R. Roy, *Chemistry*, 2008, **14**, 7490.
9.   S. Cecioni, A. Imberty and S. Vidal, *Chem Rev*, 2015, **115**, 525.
10.   J.J. Lundquist and E.J. Toone, *Chem Rev*, 2002, **102**, 555.
11.   A.M. Boukerb, A. Rousset, N. Galanos, J.B. Mear, M. Thepaut, T. Grandjean, E. Gillon, S. Cecioni, C. Abderrahmen, K. Faure, D. Redelberger, E. Kipnis, R.

Dessein, S. Havet, B. Darblade, S.E. Matthews, S. de Bentzmann, B. Guery, B. Cournoyer, A. Imberty and S. Vidal, *J Med Chem*, 2014, **57**, 10275.

12. F. Morvan, S. Vidal, E. Souteyrand, Y. Chevolot and J.J. Vasseur, *Rsc Adv*, 2012, **2**, 12043.

13. F. Casoni, L. Dupin, G. Vergoten, A. Meyer, C. Ligeour, T. Gehin, O. Vidal, E. Souteyrand, J.J. Vasseur, Y. Chevolot and F. Morvan, *Org Biomol Chem*, 2014, **12**, 9166.

14. B. Gerland, A. Goudot, C. Ligeour, G. Pourceau, A. Meyer, S. Vidal, T. Gehin, O. Vidal, E. Souteyrand, J.J. Vasseur, Y. Chevolot and F. Morvan, *Bioconjug Chem*, 2014, **25**, 379.

15. C. Ligeour, L. Dupin, A. Marra, G. Vergoten, A. Meyer, A. Dondoni, E. Souteyrand, J.J. Vasseur, Y. Chevolot and F. Morvan, *Eur J Org Chem*, 2014, **34**, 7621.

16. S. Cecioni, A. Imberty and S. Vidal, *Chem Rev*, 2015, **115**, 525.

17. C. Ligeour, L. Dupin, A. Angeli, G. Vergoten, S. Vidal, A. Meyer, E. Souteyrand, J.J. Vasseur, Y. Chevolot and F. Morvan, *Org Biomol Chem*, 2015, **13**, 11244.

18. S. Wang, L. Dupin, M. Noel, C.J. Carroux, L. Renaud, T. Gehin, A. Meyer, E. Souteyrand, J.J. Vasseur, G. Vergoten, Y. Chevolot, F. Morvan and S. Vidal, *Chemistry*, 2016, **22**, 11785.

19. F. Pertici and R.J. Pieters, *Chem Commun (Camb)*, 2012, **48**, 4008.

20. S. Cecioni, J.P. Praly, S.E. Matthews, M. Wimmerova, A. Imberty and S. Vidal, *Chemistry*, 2012, **18**, 6250.

21. C. Ligeour, O. Vidal, L. Dupin, F. Casoni, E. Gillon, A. Meyer, S. Vidal, G. Vergoten, J.M. Lacroix, E. Souteyrand, A. Imberty, J.J. Vasseur, Y. Chevolot and F. Morvan, *Org Biomol Chem*, 2015, **13**, 8433.

22. D. Sicard, S. Cecioni, M. Iazykov, Y. Chevolot, S.E. Matthews, J.P. Praly, E. Souteyrand, A. Imberty, S. Vidal and M. Phaner-Goutorbe, *Chem Commun (Camb)*, 2011, **47**, 9483.

23. D. Sicard, Y. Chevolot, E. Souteyrand, A. Imberty, S. Vidal and M. Phaner-Goutorbe, *J Mol Recognit*, 2013, **26**, 694.

24. L. Dupin, F. Zuttion, T. Gehin, A. Meyer, M. Phaner-Goutorbe, J.J. Vasseur, E. Souteyrand, F. Morvan and Y. Chevolot, *Chembiochem*, 2015, **16**, 2329.

25. M. Phaner-Goutorbe, M. Iazykov, R. Villey, D. Sicard and Y. Robach, *Mater Sci Eng C Mater Biol Appl*, 2013, **33**, 2311.

26. N. Metropolis and S. Ulam, *J Am Stat Assoc*, 1949, **44**, 335.

27. P. Derreumaux and G. Vergoten, *J Chem Phys*, 1995, **102**, 8586.

28. P. Lagant, D. Nolde, R. Stote, G. Vergoten and M. Karplus, *J Phys Chem A*, 2004, **108**, 4019.

29. S. Cecioni, S. Faure, U. Darbost, I. Bonnamour, H. Parrot-Lopez, O. Roy, C. Taillefumier, M. Wimmerova, J.P. Praly, A. Imberty and S. Vidal, *Chemistry*, 2011, **17**, 2146.

30. C. Bustamante, C. Rivetti and D.J. Keller, *Curr Opin Struct Biol*, 1997, **7**, 709.

31. M.J. Waner, M. Gilchrist, M. Schindler and M. Dantus, *J Phys Chem B*, 1998, **102**, 1649.

32. S. Cecioni, R. Lalor, B. Blanchard, J.P. Praly, A. Imberty, S.E. Matthews and S. Vidal, *Chem-Eur J*, 2009, **15**, 13232.

33. A. Pyne, R. Thompson, C. Leung, D. Roy and B.W. Hoogenboom, *Small*, 2014, **10**, 3257.

34. N.C. Santos and M.A. Castanho, *Biophys Chem*, 2004, **107**, 133.

35. R.U. Kadam, D. Garg, J. Schwartz, R. Visini, M. Sattler, A. Stocker, T. Darbre and J.L. Reymond, *ACS Chem Biol*, 2013, **8**, 1925.

36. F. Zuttion, C. Ligeour, O. Vidal, M. Walte, F. Morvan, S. Vidal, J.J. Vasseur, Y. Chevolot, M. Phaner-Goutorbe and H. Schillers, *Nanoscale*, 2018, **10**, 12771.

37. A. Dazzi, C.B. Prater, *C*hem. Rev., 2017,**117**, 75146.